Fuel Cell Electric Vehicles for Integration of Hydrogen and Electricity Systems

Alavi, Farid; van de Wouw, Nathan; De Schutter, Bart

DOI
10.1007/978-3-031-69015-0_15

Publication date
2025

Document Version
Final published version

Published in
Energy Systems Integration for Multi-Energy Systems

Citation (APA)
Alavi, F., van de Wouw, N., & De Schutter, B. (2025). Fuel Cell Electric Vehicles for Integration of Hydrogen and Electricity Systems. In C. Ocampo-Martinez, & N. Quijano (Eds.), *Energy Systems Integration for Multi-Energy Systems: From Operation to Planning in the Green Energy Context* (pp. 361-387). (Green Energy and Technology; Vol. Part F336). Springer. https://doi.org/10.1007/978-3-031-69015-0_15

Fuel Cell Electric Vehicles for Integration of Hydrogen and Electricity Systems

Farid Alavi, Nathan van de Wouw, and Bart De Schutter

1 Introduction

In this section, FCEV and their operation in the vehicle-to-grid mode are introduced. Furthermore, the concept of Car as Power Plant (CaPP) is presented, where a fleet of FCEVs is used for the task of power generation within a microgrid. This chapter is focused on the energy management system within the CaPP concept. Therefore, after introducing three different control levels in power systems, the power scheduling problem of distributed energy sources is presented and some existing methods in the literature are reviewed.

Furthermore, the developed model for the considered CaPP system and the centralized control algorithms are presented in Sect. 2. In Sect. 2.4, the development of three distributed control algorithms for the CaPP system is described. Conclusions and recommendations for future research are discussed in Sect. 4.

The control algorithms of this chapter have already been published in [1, 2]. However, this chapter is presented with the aim of elaborating the integration of hydrogen and electricity networks by using fuel cell electric vehicles in the power generation mode.

F. Alavi (✉)
Freelance Researcher, Delft, The Netherlands
e-mail: f.alavi2008@gmail.com

N. van de Wouw
Department of Mechanical Engineering, Eindhoven University of Technology, Eindhoven, The Netherlands
e-mail: n.v.d.wouw@tue.nl

B. De Schutter
Delft Center for Systems and Control, Delft University of Technology, Delft, The Netherlands
e-mail: b.deschutter@tudelft.nl

C. Ocampo-Martinez and N. Quijano (eds.), *Energy Systems Integration for Multi-Energy Systems*, Green Energy and Technology, https://doi.org/10.1007/978-3-031-69015-0_15

1.1 Fuel Cell Electric Vehicles

In fuel cell electric vehicles (FCEVs), the drivetrain power is generated by a fuel cell stack. Depending on the electric drivetrain technology, the electric motors in FCEVs can be of alternating current (AC) or direct current (DC) technology. Power electronic systems, such as voltage converters or inverters, are used to control the electric motors, battery, and fuel cell stack. Even though the presence of a battery makes the structure of an FCEVs similar to that of Battery Electric Vehicles (BEVs), they differ in the size of their battery bank and the presence of a fuel cell system.

An FCEV requires a much smaller battery compared to a BEV. Namely, an FCEV is equipped with a fuel cell system that provides almost all the energy that the vehicle requires. Therefore, in contrast to a BEV, the battery of an FCEV is not the main energy source and it is mainly used for providing extra power when there is a need for rapid acceleration. Note that there is a type of BEVs in which the fuel cell system is used as a range extender of the vehicle [3]. In this specific type of vehicles, the fuel cell stack is smaller and the battery is larger compared to a normal FCEV. In fact, these type of vehicles can be considered as a BEV with an onboard charging system based on fuel cell technology. In this chapter, we consider a normal fuel cell vehicle, i.e., a vehicle in which the main power source is a fuel cell stack.

The fuel cell stack is used to convert chemical energy present in hydrogen into electricity. This conversion in the form of energy is a result of a chemical reaction inside the fuel cell as follows [4]:

$$2H_2 + O_2 \rightarrow 2H_2O. \tag{1}$$

The chemical reaction (1) is in fact the process of burning hydrogen. However, in a fuel cell system, this chemical reaction is realized in a specific manner, in which the electrons of the hydrogen molecules are separated from their respective protons at the beginning of the process. This step is done by using a membrane that only allows the protons to pass through. As the protons pass through the membrane and reach the other side of the membrane, i.e., the cathode, these react with the oxygen (O_2) in the air and new molecules of water are created. The extra electrons required for this chemical reaction are provided by the existing electrons in the cathode plate. Therefore, the whole process results in a shortage of electrons at one side, i.e., the cathode side, and an excess of electrons at the other side, i.e., the anode side. Consequently, these two sides will have a difference in their electrical potential and a flow of electrons, or electrical current, will occur if there is an electrical circuit outside of the fuel cell connecting the anode and cathode.

The source of energy in FCEVs is hydrogen and it is stored in a gaseous state using a high-pressure tank inside the vehicle. The typical pressure of the gas in such storage tanks is around 700 bar. With this pressure, a tank with a normal volume of around 122 liter can provide almost 5 kg of hydrogen, which is sufficient to drive a car for about 500 km. Even though these numbers can depend on the specific design of the vehicle, it is important to point out that with the current level of technology,

FCEVs can be built and used on the road efficiently. Examples of such FCEVs are the Hyundai NEXO, the Toyota Mirai, the Honda Clarity, and the Mercedes-Benz F-Cell. Even though hydrogen is an explosive gas, the safety level of FCEVs is high, thanks to a conservative design of the hydrogen tanks. A recent study [5] shows that FCEVs are accepted as a safe type of vehicle and [6] argues that FCEVs will be more common in the future. The aforementioned commercial models of FCEVs have passed the required level of certification to be used on public roads in Europe. A hydrogen tank can be fully charged in less than 5 min, and this fast charging procedure combined with the relatively long driving range is an advantage of FCEVs compared to BEVs.

1.2 Car as Power Plant

In recent years, there has been a trend of incorporating more Renewable Energy Sources (RESs) into the power grids. Specific features of this relatively new source of electricity generation will change the shape of energy systems in the future [7]. Uncertainty in power generation is one specific feature of RESs that have the sun or wind as their source of energy. In addition to that, these types of RESs are not dispatchable. As a result, a power grid with a high share of RESs requires flexibility sources, i.e., power generation or storage units with highly controllable operating power, as well [8, 9].

Connecting BEVs to the power grid via vehicle-to-grid (V2G) technology creates flexibility required for future electric power systems. Smart charging strategies of the BEVs are developed to assist in achieving a smooth overall power demand profile of the network [10]. Additionally, the batteries of BEVs allow the power network operators to store surplus power generated by RESs.

FCEVs can potentially assist the realization of power systems with a high share of RESs. This type of vehicle, with hydrogen as fuel, can be utilized to provide peak power or spinning reserves to the grid [11, 12]. While in BEVs the input and output are in the form of electricity and the vehicle is in essence an electrical load and a medium of storing energy in grid-connected mode, FCEVs use hydrogen as their source of energy and their output energy is in the form of electricity. As FCEVs are used both in transportation and electrical power generation, this type of vehicle creates a link between hydrogen and electricity networks [13].

This chapter adopts the CaPP concept [14]. In a CaPP scenario, FCEVs are utilized as dispatchable power plants, thereby creating a flexible multi-modal energy system [15]. Considering that FCEVs can generate electricity from hydrogen in a clean and efficient manner and, considering that cars are used for driving only around 5% of the time [14], a large fleet of FCEVs can be utilized as a power plant.

This chapter focuses in particular on the power scheduling problem of a CaPP system inside a residential islanded-mode microgrid. Hydrogen is used by FCEVs as a fuel for transportation, as well as a source of energy in the power generation mode. The power generated by FCEVs can assist the power balance of the microgrid when

power generated by RESs is scarce. The perspective of this chapter is from operational control, as it is one of the main challenges in implementing such microgrids [16].

The power scheduling of the FCEVs is an aspect of operational control of a CaPP microgrid that is considered in this chapter. In the literature, usually centralized planning algorithms are used for power scheduling of a hydrogen-based microgrid [17]. Robust optimization and stochastic programming are common methods to deal with the uncertainty in power planning of microgrids [18, 19]. Depending on the specific application, the cost function of the optimization-based control method can be the power losses [20], operational costs [21], or the imported power to the microgrid [22]. Simpler control strategies are used in another source [23], where the sizing of the solar photovoltaic (PV) panels and techno-economic aspects of a PV-to-hydrogen system with fuel cell buses are studied. Note that control of FCEVs in a CaPP system differs from the aforementioned applications in the sense that it considers two operational modes for the FCEVs, namely, power generation and transportation.

1.3 Energy Management Systems

In operating any microgrid, maintaining the power balance is of high importance. Traditionally, three control levels are used in control of power systems, called primary, secondary, and tertiary control levels. While the objective of the first two levels is regularization of the voltage and frequency of the power system [24–26], tertiary control [27] aims to determine suitable power generation profiles for each generator in the system. In determining the power generation profiles in the tertiary control level, the operational cost of the system is minimized, while the physical constraints of the system, such as the energy balance and the power generation capacity of each generator are taken into account. The focus of this chapter is on the tertiary control, i.e., power generation profiles of FCEVs are determined in such a way that the operational costs are minimized and the physical constraints of the system are satisfied.

The control system that manages the demand and production of the electricity in a smart grid, of which the distributed power generation based on FCEVs is an example, is called an energy management system. Several works have considered controller design for such systems. In [28], the problem of charging and discharging of BEVs in a smart grid is considered in order to reach a power balance in the system and gain the maximum operational benefit. Two optimization-based methods are proposed, a centralized and a decentralized scheme. However, the developed distributed solution requires the exchange of solutions for each agent during several iterations. Therefore, the amount of communication needed is typically high in this approach.

1.3.1 Model Predictive Control in Energy Management Systems

Due to its intrinsic robustness features and its ability to deal with the constraints in the system, Model Predictive Control (MPC) is an advanced control method that has gained much attention in design of an energy management system for smart grid applications. Regarding the work [29], a distributed MPC method to operate a microgrid is developed. The problem of power scheduling in a microgrid is reviewed in [30–32]. Another example of using MPC in the operation of a microgrid system is [33], where it is assumed that the controlled microgrid has a renewable energy source, a storage battery system, and some electrical loads. The designed control algorithm is based on an optimization problem that takes into account the cost of system operation. However, [33] neglects binary variables that determine different operational modes of devices and, hence, some part of the operational cost is not considered.

The work presented in [34], control of a microgrid that contains several power plants, a photovoltaic system, and a fuel cell system is considered. The problem is formulated using Mixed-Logical Dynamical (MLD) models and the optimization problem is solved with multiparametric programming techniques. Another example of using MPC for control of microgrids that contain fuel cells and solar photovoltaic systems is [35]. In that paper, a method is developed to control the system via market trades, involving a mechanism of bidding and auctions to balance the system based on electricity prices. However, the developed method cannot guarantee the stability of the system.

The design of an MPC controller in order to operate several devices in a smart grid is discussed in [36]. In that paper, the optimization problem is expressed as a mixed integer linear programming problem. However, [36] assumes that the future load profile is predetermined and that there is no uncertainty in the system.

The prediction of the load in a microgrid is not ideal and contains uncertainty. In order to deal with this uncertainty in the energy management systems, robust control techniques are used in [37–39]. A stochastic optimization approach for the energy management system is developed in [39], while in [37, 38] min-max formulations are used. In [40], a method is developed to model the uncertainty in power systems as a polytope, while an appropriate control strategy to deal with the modeled uncertainty is not discussed.

Three different methods to deal with the uncertainty in the power systems are discussed in [41]. The first method simply considers some power generation units in the standby operation mode in order to provide excess electricity if it is needed. The second method uses stochastic optimization in order to set an appropriate power production profile for each generator. However, this method requires a priori knowledge about the uncertainties in the system. The last method employs robust optimization, which guarantees the stability of the system in presence of all the possible disturbances. The advantage of the third method compared to the second method is that accurate information about the uncertainties is not necessary.

Min-max MPC and stochastic MPC [42] are two widely used optimization-based control methods for dealing with uncertainty in power networks. An advantage of

using min-max MPC compared to stochastic MPC is that we only need to determine an interval for the realization of the uncertainty; no extra information about the uncertain parameters, such as the probability distribution functions, is needed. Even though the min-max MPC method has the advantage of simplicity, it suffers from a high level of conservatism, meaning that the actual operational cost may be higher than that of a typical MPC method using a nominal model. On the other hand, min-max MPC guarantees the satisfaction of constraints in the system. For applications where the system's stability is of utmost importance at all times, such as in our case for balancing the power in microgrids, min-max MPC is a suitable choice.

Fortunately, there are remedies to reduce the conservatism of the min-max approach. For instance, [43] has developed a method called min-max disturbance feedback. In that method, a feedback law is incorporated into the control system, accounting for model uncertainty. Consequently, min-max MPC becomes less conservative and more suitable for real-world applications. In a similar concept, [44] shows that the feedback on the disturbance creates a set of possible state trajectories in the form of a tube across the state-space.

The control methods mentioned above focus on designing a controller with a centralized architecture, in which there is a single controller that receives all the information of the system and that determines the control inputs for all the agents in the system. An agent here refers to a single FCEV connected to the microgrid. An alternative solution involves a distributed architecture, in which several agents inside the system interact to determine the control inputs of the system. A distributed control architecture can be used to reduce the computational complexity of the optimization problem in MPC controllers. In this method, the optimization problem is reformulated as several smaller optimization problems and each problem is solved separately. Dual decomposition [45] and the alternating direction method of multipliers (ADMM) [46] are two well-known methods in distributed control. An alternative method is called proximal ADMM [47], where a proximal term is added to the cost function of the dual problem and a result is the faster convergence toward the solution. However, these methods have been originally developed for convex programming problems. Using these methods to solve a non-convex optimization problem may result in a suboptimal solution, because of a duality gap between primal and dual problems [45]. If the distributed generation units inside a microgrid have ON/OFF switching signals, binary variables are introduces to the optimization problem and, hence, the energy management system will face such a non-convex optimization problem for power scheduling of the generation units. As a result, conventional distributed control methods might be inefficient.

As discussed above, robust and distributed control algorithms are already available in the literature. However, the unique features of the CaPP system require specialized algorithms, which we develop in this chapter. The primary contribution of our work is the development of several robust MPC strategies for the CaPP system. Two of these strategies have a centralized architecture, while the other three are distributed. The three distributed robust MPC controllers are superior to the existing methods in the literature in the sense that the driving patterns of the FCEVs are not shared with the controller. Additionally, [1] demonstrates that the distributed methods exhibit

acceptable performance for a large fleet of vehicles. Furthermore, we formulate the power scheduling problem, taking into account specific features of the system, such as driving patterns, vehicle refueling processes, and the privacy of FCEV owners.

2 Model Predictive Control of Smart Energy Systems with FCEVs

2.1 System Description

An islanded-mode microgrid is considered that includes RESs, such as solar PV cells and wind turbines, a fleet of FCEVs in the V2G mode, and diesel generators. It is assumed that the load of the microgrid is not controllable. Therefore, the power balance of the microgrid is maintained by altering the power generation profile of the generation units. The goal of the system is to use diesel generators as little as possible. Consequently, the objective of the controller is to determine a suitable power generation profile for each FCEV such that the power balance of the microgrid is maintained and the operational cost of the system is minimized.

The control algorithm adopted in this chapter is similar to a traditional tertiary control algorithm in the sense that both algorithms have the objective of minimizing the operational cost of the system with respect to the system constraints. However, the system considered in this chapter has some unique features that necessitate the design of a new control system. Among these features are the dual usage of the generation units—in transportation and power generation modes—limited fuel in each FCEV, and unavailability of an FCEV during the refueling process. As mentioned before, the details of the control algorithms of this chapter are reported in [1].

The efforts of the primary and secondary control levels to regulate the frequency and voltage of the power system result in an actual power generation profile that can be different from the scheduled profile. In the scenario of this chapter, it is assumed that each FCEV is also equipped with these two control levels. Hence, there is a mismatch between the scheduled and the actual power generation profile for each FCEV, which is considered as an uncertain parameter here. In order to deal with this uncertainty, robust power scheduling algorithms are developed for the tertiary control level.

In the scenario considered here, each FCEV is equipped with a computing unit that can communicate with a central control system. For the sake of simplicity, it is assumed that the communication is ideal, meaning that there is no delay, packet loss, or cost in the exchange of information. Additionally, it is also assumed that whenever an FCEV is not used for transportation or refueling, it is connected to the microgrid.

2.2 Mixed Logical Dynamical Model of the System

The remaining fuel in each FCEV is considered as a system state. Therefore, the system states can change both in the transportation and the power generation mode. The transportation mode of each vehicle is determined by the driving pattern of the vehicle owner. We assume that by studying the behavior of each driver, it is possible to determine the driving pattern of each driver for a prediction window from the current time step k to a future time step $k + N_{\mathrm{p}}$, where N_{p} is called the prediction horizon. By defining $\mathcal{P} = \{0, 1, \ldots, N_{\mathrm{p}} - 1\}$ and $\mathcal{I} = \{1, \ldots, N_{\mathrm{veh}}\}$ with N_{veh} the total number of vehicles in the system, we can model the availability of a vehicle $i \in \mathcal{I}$ for power generation at time step $k + j$, for each $j \in \mathcal{P}$, with a sequence of binary variables $\lambda_{\mathrm{f},i}(k + j)$ for $i \in \mathcal{I}$ and $j \in \mathcal{P}$: if FCEV i is in the transportation mode at time step $k + j$, then $\lambda_{\mathrm{f},i}(k + j)$ is equal to 1, and otherwise it is 0. In addition, we assume that if a vehicle arrives at the geographical area of the microgrid in the period $\big[(k - 1)T_{\mathrm{s}}, kT_{\mathrm{s}}\big)$, with T_{s} the sampling interval, then the amount of fuel that is used for that trip is predictable and described by $h_{\mathrm{f},i}(k)$. Therefore, we can assume that if a vehicle is in the transportation mode, the fuel level remains the same, and at the time step k, i.e., the next time step after the arrival, it will be reduced with the amount $h_{\mathrm{f},i}(k)$. We also consider a specific mode for refueling a vehicle where the fuel level is increased by $R_{\mathrm{f},i}$ at each time step.

By considering the relation between the fuel consumption and the net power generation of a fuel cell [48], we can derive the following equation for the evolution of the fuel level of vehicle $i \in \mathcal{I}$ in the power generation mode:

$$x_{\mathrm{f},i}(k + 1) = x_{\mathrm{f},i}(k) - (\alpha_{\mathrm{f},i} u^*_{\mathrm{f},i}(k) + \beta_{\mathrm{f},i})T_{\mathrm{s}}, \tag{2}$$

where $\alpha_{\mathrm{f},i}$ and $\beta_{\mathrm{f},i}$ are parameters related to the fuel cell i and T_{s} is the sampling time interval. The actual power generation of fuel cell i at time step k is indicated by $u^*_{\mathrm{f},i}(k)$. Considering the fact that the primary and secondary controllers may induce actual power generation levels that deviate from the scheduled level, we have

$$u^*_{\mathrm{f},i}(k) = u_{\mathrm{f},i}(k) + d_i(k), \tag{3}$$

where $u_{\mathrm{f},i}(k)$ indicates the scheduled power generation of fuel cell $i \in \mathcal{I}$ at time step k and $d_i(k)$ is an unknown time-varying deviation from the scheduled value.

By gathering all the operational modes of FCEV $i \in \mathcal{I}$, the following model is developed:

$$x_{\mathrm{f},i}(k + 1) = \begin{cases} x_{\mathrm{f},i}(k) + R_{\mathrm{f},i} & \text{refueling} \\ x_{\mathrm{f},i}(k) & \text{inactive} \\ x_{\mathrm{f},i}(k) - (\alpha_{\mathrm{f},i} u^*_{\mathrm{f},i}(k) + \beta_{\mathrm{f},i})T_{\mathrm{s}} & \text{generation} \\ x_{\mathrm{f},i}(k) & \text{transportation} \\ x_{\mathrm{f},i}(k) - h_{\mathrm{f},i}(k) & \text{arrival} \end{cases} \tag{4}$$

To indicate the operational mode of FCEV $i \in \mathcal{I}$, we use two binary variables $s_{\mathrm{f},i}$ and $s_{\mathrm{r},i}$. The refueling mode at time step k is indicated by $s_{\mathrm{r},i}(k) = 1$; in other modes, we have $s_{\mathrm{r},i}(k) = 0$. The power generation mode corresponds to $s_{\mathrm{f},i}(k) = 1$ and, if $s_{\mathrm{f},i}(k) = 0$, the fuel cell i is turned off. It is assumed that while an FCEV is in the driving mode, it can neither generate power for the microgrid nor be refilled. These constraints can be represented by

$$\begin{aligned} &\text{if } \lambda_{\mathrm{f},i}(k) = 1 \text{ then } s_{\mathrm{r},i}(k) = 0, \\ &\text{if } \lambda_{\mathrm{f},i}(k) = 1 \text{ then } s_{\mathrm{f},i}(k) = 0. \end{aligned}$$

We assume that if a fuel cell is being refilled, it cannot generate power. Other constraints in the operation of a fuel cell include the maximum level of power generation and the maximum fuel level. Moreover, a fuel cell can generate power only when the fuel level of the vehicle is above a certain minimum level. These constraints can be represented as follows:

$$\begin{aligned} &\text{if } s_{\mathrm{r},i}(k) = 1 \text{ then } s_{\mathrm{f},i}(k) = 0, \\ &0 \le u_{\mathrm{f},i}(k) \le \bar{u}_{\mathrm{f},i}, \\ &\underline{x}_{\mathrm{f},i} s_{\mathrm{f},i}(k) \le x_{\mathrm{f},i}(k) \le \bar{x}_{\mathrm{f},i}. \end{aligned}$$

The equivalent MLD model [49] of the system in (4) with the constraints as explained above is given by

$$\begin{aligned} &\mathbf{x}(k+1) = \mathbf{x}(k) + B_1(d(k))\mathbf{u}(k) + B_3(k)\mathbf{z}(k) + B_4(k), \\ &E_1\mathbf{u}(k) + E_4\mathbf{x}(k) + E_5(k) \ge E_3\mathbf{z}(k), \end{aligned} \tag{5}$$

where the vectors $\mathbf{x}(k)$, $\mathbf{u}(k)$, and $\mathbf{z}(k)$ are defined as

$$\begin{aligned} \mathbf{x}(k) &= \left[x_{\mathrm{f},1}(k) \ \dots \ x_{\mathrm{f},N_{\mathrm{veh}}}(k) \right]^T, \\ \mathbf{u}(k) &= \left[u_{\mathrm{f},1}(k) \ s_{\mathrm{r},1}(k) \ s_{\mathrm{f},1}(k) \ \dots \ u_{\mathrm{f},N_{\mathrm{veh}}}(k) \ s_{\mathrm{r},N_{\mathrm{veh}}}(k) \ s_{\mathrm{f},N_{\mathrm{veh}}}(k) \right]^T, \\ \mathbf{z}(k) &= \left[z_{\mathrm{f},1}(k) \ \dots \ z_{\mathrm{f},N_{\mathrm{veh}}}(k) \right]^T. \end{aligned} \tag{6}$$

2.3 Centralized Robust Control for a CaPP System

In this section, two centralized robust MPC approaches are developed by considering the specific features of the system, such as the presence of some fuel cell stacks that are used both for power generation and for transportation.

Min-Max Control Method

The model for the system developed in Sect. 2.2 contains an uncertain variable, d_i, $i \in \mathcal{I}$, see (3), and to deal with this uncertainty, a min-max control method is proposed here. In the min-max control method, the operational cost of the system is minimized for the worst-case realization of the uncertainty. In addition, by satisfying the system constraints for the worst-case uncertainty, the min-max control method guarantees the satisfaction of the constraints for any realization of the uncertainty.

We can define the following cost function for the system [2]:

$$J(k) = \sum_{j \in \mathcal{P}} \sum_{i \in \mathcal{I}} \left[W_{\mathrm{p},i} u_{\mathrm{f},i}^2(k+j) + W_{\mathrm{s},i} |\Delta s_{\mathrm{f},i}(k+j)| + C_{\mathrm{e}}(k+j) d_i(k+j) \right], \tag{7}$$

where $\Delta s_{\mathrm{f},i}(k+j)$ is defined as $s_{\mathrm{f},i}(k+j) - s_{\mathrm{f},i}(k+j-1)$. The two parameters, $W_{\mathrm{p},i}$ and $W_{\mathrm{s},i}$, determine the cost of power generation and the cost of switching the operational mode of a fuel cell. The value of $d_i(k+j)$ indicates the deviation from the scheduled power generation of fuel cell $i \in \mathcal{I}$ at time step $k+j$. This deviation is the result of an effort for stabilizing the microgrid. In order to encourage the FCEVs to stabilize the microgrid, we assume that each fuel cell $i \in \mathcal{I}$ gets a reward equal to $C_{\mathrm{e}}(k+j) d_i(k+j)$ at time step $k+j$ for the willingness to deviate its actual power generation from the scheduled one by the amount of $d_i(k+j)$. This reward for FCEVs is an additional cost for the microgrid operator. We consider a predetermined value for this additional cost for each unit of power generation and hence the last term of (7) has a linear form with respect to the deviation d_i.

Define

$$\begin{aligned} \mathbf{d}_i(k) &= \left[d_i(k) \ \ldots \ d_i(k+N_{\mathrm{p}}-1) \right]^T, \\ \mathbf{V}_i(k) &= \left[\tilde{\mathbf{u}}_i^T(k) \ \tilde{\mathbf{z}}_i^T(k) \right]^T, \end{aligned} \tag{8}$$

where the vectors $\tilde{\mathbf{u}}_i$ and $\tilde{\mathbf{z}}_i$ in (8) are the stacked version of $\mathbf{u}_i$ and $\mathbf{z}_i$ over time steps k to $k+N_{\mathrm{p}}-1$, where

$$\begin{aligned} \mathbf{u}_i(k) &= \left[u_{\mathrm{f},i}(k) \ s_{\mathrm{r},i}(k) \ s_{\mathrm{f},i}(k) \right], \\ z_i(k) &= s_{\mathrm{f},i}(k) u_{\mathrm{f},i}(k). \end{aligned}$$

Using the above definitions, the operational cost of the system can be rewritten as

$$J(k) = \sum_{i \in \mathcal{I}} \left(\mathbf{V}_i^T(k) W_{\mathrm{q},i}(k) \mathbf{V}_i(k) + W_{\mathrm{v},i}(k) \mathbf{V}_i(k) + W_{\mathrm{d},i}(k) \mathbf{d}_i(k) \right), \tag{9}$$

where $W_{\mathrm{q},i}$, $W_{\mathrm{v},i}$, and $W_{\mathrm{d},i}$ can be determined for all $i \in \mathcal{I}$ based on the values of $W_{\mathrm{p},i}$, $W_{\mathrm{s},i}$, and C_{e}, respectively. The vector of optimization variables, $\mathbf{V}(k)$, is defined as

$$\mathbf{V}(k) = \left[\, \mathbf{V}_1^T(k) \ \ldots \ \mathbf{V}_{N_{\text{veh}}}^T(k) \,\right]^T, \tag{10}$$

By extending the system constraints in (5) to all the time steps in the prediction window, we can determine matrices $G_{1,i}$, $G_{2,i}$, and $G_{3,i}$ such that the following inequalities describe the system constraints in the whole prediction window:

$$G_{1,i}(\mathbf{d}_i(k))\mathbf{V}_i(k) \leq G_{2,i}(k) + G_{3,i}(k)x_i(k), \ \forall i \in \mathcal{I}. \tag{11}$$

The power balance condition is:

$$\sum_{i \in \mathcal{I}} u_{\text{f},i}(k+j) = P_{\text{d}}(k+j), \ \forall j \in \mathcal{P}, \tag{12}$$

where $P_{\text{d}}(k+j)$ is the residual load of the microgrid at time step $k+j$, i.e., the microgrid's load minus the generated power by the renewable energy sources. The inequalities (11) and equalities (12) include all the operational constraints of the system.

In the min-max approach, the aim is to minimize the operational cost of the system for the worst-case uncertainty, while the system constraints are satisfied for any realization of the uncertainty. So, the following optimization problem should be solved at each time step k:

$$\begin{aligned} \min_{\{\mathbf{V}_i(k)\}_{i\in\mathcal{I}}} \max_{\{\mathbf{d}_i(k)\}_{i\in\mathcal{I}}} \sum_{i\in\mathcal{I}} \big(\mathbf{V}_i^T(k) W_{\text{q},i}(k)\mathbf{V}_i(k) + W_{\text{v},i}(k)\mathbf{V}_i(k) \\ + W_{\text{d},i}(k)\mathbf{d}_i(k)\big) \\ \text{subject to (11), (12), for all } \mathbf{d}_i \text{ where } i \in \mathcal{I}. \end{aligned} \tag{13}$$

We assume that the uncertainties are always realized within given bounds as follows:

$$\text{d}_{i,\min} \leq d_i(k) \leq \text{d}_{i,\max}, \ \text{for all } i \in \mathcal{I} \text{ and } k. \tag{14}$$

The source of uncertainty is the errors in the prediction of the residual load, which contain the errors in the prediction of RES power generation and the microgrid's load. Note that because the microgrid is operated in the islanded mode, the total power generation of FCEVs is equal to the residual load and, hence, the inaccuracy in the prediction of the residual load results in the presence of the uncertain parameters $d_i(k)$ for $i \in \mathcal{I}$. An extensive review on the different methods of forecasting the load is presented in [50] and based on this reference, a common forecasting method can be written in the form $p(k) = f(k) + v(k)$, where $p(k)$ is the predicted load, $f(k)$ is the value of a predetermined function, and $v(k)$ is a bounded noise at time step k. Because the uncertain variables $d_i(k)$ for all $i \in \mathcal{I}$ are proportionally related to the error in the total load of the microgrid, we can define a minimum and a maximum level for realization of each $d_i(k)$.

As a result of (14), we can define the set $\mathcal{D}$ such that

$$\tilde{\mathbf{d}}(k) = [\mathbf{d}_1^T(k) \ \ldots \ \mathbf{d}_{N_{\text{veh}}}^T(k)]^T \in \mathcal{D},$$

where for all $i \in \mathcal{I}$, all the elements of $\mathbf{d}_i(k)$ comply with the inequalities in (14).

By using Lemma 5.3.1 of [51], the optimization problem (13) can be rewritten as follows:

$$\begin{aligned} \min_{\mathbf{V}_i(k), i\in\mathcal{I}} \ \max_{p\in\{1,\ldots,N\}} \ & \sum_{i\in\mathcal{I}} \big(\mathbf{V}_i^T(k) W_{\text{q},i}(k)\mathbf{V}_i(k) \\ & + W_{\text{v},i}(k)\mathbf{V}_i(k) + W_{\text{d},i}(k)\hat{\mathbf{d}}_{p,i}(k)\big) \\ \text{subject to (11) and (12).} & \end{aligned} \tag{15}$$

The problem (15) is a mixed integer quadratic programming (MIQP) problem and can be solved by a standard solver such as CPLEX [52] or Gurobi [53].

Disturbance Feedback Min-Max Control Method

The min-max control method of Sect. 2.3 guarantees that the system constraints are satisfied for any realization of the disturbance in the power demand of the microgrid. However, the level of conservatism in the min-max method may be considerable. In this section, an alternative method, called disturbance feedback min-max control, is developed by using the idea of [43]. Even though the realized value of the disturbance is unknown to the controller, the presence of a disturbance feedback mechanism prevents the expansion of possible state trajectories in the prediction horizon. As a result, the disturbance feedback min-max controller is less conservative compared to the regular min-max controller of Sect. 2.3.

In the disturbance feedback min-max approach, a control law is considered for the sequence of future control inputs of FCEVs. For each time step $k + j$, the control input of FCEV i is determined as follows:

$$u_{\text{f},i}(k+j) = v_{\text{f},i}(k+j) + K_{\text{f},i}(k+j)d_i(k+j-1), \ \forall i \in \mathcal{I}, \tag{16}$$

where $v_{\text{f},i}(k+j)$ and $K_{\text{f},i}(k+j)$ are, respectively, the deterministic part of the scheduled power generation and the disturbance feedback gain for FCEV $i \in \mathcal{I}$ at time step $k + j$. The value of $d_i(k + j - 1)$ is unknown before time step $k + j$, but after that it can be determined by subtracting the actual power generation, $u_{\text{f},i}^*(k + j - 1)$ from the scheduled power generation, $u_{\text{f},i}(k + j - 1)$. Note that in the disturbance feedback method, the scheduled power generation, $u_{\text{f},i}(k + j)$, at time step $k + j$ for $j \geq 1$ consists of two parts: a deterministic part, i.e., $v_{\text{f},i}(k + j)$, and an unknown part, i.e., $K_{\text{f},i}d_i(k + j - 1)$. The value of the deterministic part of the scheduled power generation, $v_{\text{f},i}$, and the feedback gain, $K_{\text{f},i}$, are determined via solving an optimization problem for all $i \in \mathcal{I}$.

Using (16), the actual power generation of FCEVs can be still represented by (3). In addition, the model of FCEVs will remain the same. However, the matrices B_3 and E_1 in (5) will become functions of $d(k-1)$. The resulting MLD model is of the form

$$\begin{aligned} &\mathbf{x}(k+1) = \mathbf{x}(k) + B_1(d(k))\mathbf{u}(k) + B_3(d(k-1))\mathbf{z}(k) + B_4(k) \\ &E_1(d(k-1))\mathbf{u}(k) + E_4\mathbf{x}(k) + E_5(k) \geq E_3\mathbf{z}(k), \end{aligned} \tag{17}$$

where the definition of $\mathbf{x}$ remains the same as in (6). The new definition of $\mathbf{u}$ and $\mathbf{z}$ is as follows:

$$\begin{aligned} \mathbf{u}(k) &= [v_{\mathrm{f},1}(k)\ s_{\mathrm{r},1}(k)\ s_{\mathrm{f},1}(k)\ K_{\mathrm{f},1}(k)\ \ldots\ v_{\mathrm{f},N_{\mathrm{veh}}}(k)\ s_{\mathrm{r},N_{\mathrm{veh}}}(k)\ s_{\mathrm{f},N_{\mathrm{veh}}}(k)\ K_{\mathrm{f},N_{\mathrm{veh}}}(k)]^T \\ \mathbf{z}(k) &= [z_{\mathrm{f},1}(k)\ z_{\mathrm{k},1}(k)\ \ldots\ z_{\mathrm{f},N_{\mathrm{veh}}}(k)\ z_{\mathrm{k},N_{\mathrm{veh}}}(k)]^T. \end{aligned} \tag{18}$$

The variable $K_{\mathrm{f},i}(k)$ represents the disturbance feedback gain for FCEV i at time step k and the new auxiliary variables are defined as $z_{\mathrm{k},i}(k) := K_{\mathrm{f},i}(k)s_{\mathrm{f},i}(k)$ for all $i \in \mathcal{I}$. By extending the inequality constraints in (17) over the prediction horizon we obtain

$$G^{\mathrm{DF}}_{1,i}(\mathbf{d}_i(k))\mathbf{V}^{\mathrm{DF}}_i(k) \leq G^{\mathrm{DF}}_{2,i}(k) + G^{\mathrm{DF}}_{3,i}(k)x_i(k), \tag{19}$$

where $\mathbf{V}^{\mathrm{DF}}_i(k)$ has the same definition as $\mathbf{V}_i(k)$ in (8). Alavi [51] shows that (19) can be expressed in the form of linear inequalities.

The power balance constraint in the disturbance feedback min-max method can be expressed as

$$\begin{aligned} &\sum_{i\in\mathcal{I}} u_{\mathrm{f},i}(k) = P_{\mathrm{d}}(k), \\ &\sum_{i\in\mathcal{I}} v_{\mathrm{f},i}(k+j) = P_{\mathrm{d}}(k+j),\ \ j \in \{1,\ldots,N_{\mathrm{p}}-1\}. \end{aligned} \tag{20}$$

The optimization problem of the MPC controller at time step k can be written as

$$\begin{aligned} \min_{\mathbf{V}^{\mathrm{DF}}_i(k), i\in\mathcal{I}}\ \max_{p\in\{1,\ldots,N\}}\ \sum_{i\in\mathcal{I}} \Big(&(\mathbf{V}^{\mathrm{DF}}_i)^T(k) W^{\mathrm{DF}}_{\mathrm{q},i}(k)\mathbf{V}^{\mathrm{DF}}_i(k) + W^{\mathrm{DF}}_{\mathrm{v},i}(k)\mathbf{V}^{\mathrm{DF}}_i(k) \\ &+ W^{\mathrm{DF}}_{\mathrm{d},i}(k)\hat{\mathbf{d}}_{p,i}(k) \Big) \end{aligned} \tag{21}$$

subject to (19) and (20),

where $W^{\mathrm{DF}}_{\mathrm{q},i}(k)$, $W^{\mathrm{DF}}_{\mathrm{v},i}(k)$, and $W^{\mathrm{DF}}_{\mathrm{d},i}(k)$ are defined based on the cost function (7). The optimization problem (21) is an MIQP problem and a standard solver, such as CPLEX [52] or Gurobi [53], can be used to solve it.

In the disturbance feedback min-max approach, a feedback law on the future disturbances prevents the expansion of the possible state trajectories inside the predicted

period and, as a result, the level of conservatism is lower compared to the min-max method [54]. However, in order to implement these methods, the driving patterns of all the FCEVs should be shared with a central controller. To increase the privacy level of the FCEV owners, three distributed control methods are developed in the next section.

2.4 Distributed Robust Control for a CaPP System

In this section, three distributed control strategies based on the dual decomposition, the alternating direction method of multipliers (ADMM), and the proximal ADMM (PADMM) are developed in order to support the min-max and the disturbance feedback min-max approaches in a distributed fashion. In the developed methods, the driving patterns of the FCEVs are kept private, i.e., there is no need to share the information about the departure or arrival time of the FCEVs with any other agent.

The generic distributed control strategies employed in this section were originally developed for convex programming problems [45–47]. The presence of binary variables makes the optimization problems (15) and (21) non-convex and, hence, the developed algorithms might not converge at all or they might converge to a non-optimal point. The lack of convergence in the power scheduling process will result in an imbalance in the power generation and usage in the microgrid. However, the use of some diesel generators as backup generation units and some batteries to store energy can still guarantee the power balance condition of the microgrid. To decrease the use of fossil fuels or batteries, we assume that the correction of power scheduling using backup generation and storage units is much more expensive compared to the generated power of a fuel cell. Therefore, an efficient control system minimizes the use of the backup generation or storage units to decrease the operational cost of the system.

The developed methods are based on iterations, i.e., an information exchange process between a coordinator and the FCEVs. At the end of each iteration, the control system reaches a specific power schedule. If the power balance is satisfied or a maximum number of iterations is reached, the iteration process is terminated by the coordinator and the FCEVs generate the amount of power scheduled in the last iteration point; otherwise, the coordinator starts a new iteration. The backup generation and storage units are used when the iteration process is terminated while the power balance condition is not yet reached.

Dual Decomposition Method

In the dual decomposition approach, a new optimization problem, called the dual problem, is constructed based on the original problem, i.e., the primal problem, e.g., (15) or (21). In some cases, the structure of the dual problem allows us to solve it

in a distributed fashion. As will be explained below, the dual problems of (15) and (21) can be separated across all the FCEVs.

In the dual decomposition method, the dual problem is solved in a distributed fashion. Because the optimization problems are not convex, the optimum value of the dual problem might be smaller than that of the primal problem. In other words, there might be a duality gap [45]. The presence of a duality gap means that the power scheduling process has not reached the balance condition yet; in this case, the backup generation and storage units will be used to guarantee the power balance condition.

The min-max problem (15) consists of N MIQP problems, where the pth MIQP problem is formulated as the following primal problem P:

$$\begin{aligned} \mathrm{P}: \min_{\mathbf{V}_i(k), i\in\mathcal{I}} & \sum_{i\in\mathcal{I}} \left(\mathbf{V}_i^T(k) W_{\mathrm{q},i}(k)\mathbf{V}_i(k) + W_{\mathrm{v},i}(k)\mathbf{V}_i(k) + W_{\mathrm{d},i}(k)\hat{\mathbf{d}}_{p,i}(k)\right) \\ & \text{subject to (11) and (12),} \end{aligned} \tag{22}$$

and its dual problem D can be written as

$$\begin{aligned} \mathrm{D}: \max_{\lambda(k)\in\mathbb{R}^{N_\mathrm{p}}} \min_{\mathbf{V}_i(k), i\in\mathcal{I}} & \sum_{i\in\mathcal{I}} \left(\mathbf{V}_i^T(k) W_{\mathrm{q},i}(k)\mathbf{V}_i(k) + W_{\mathrm{v},i}(k)\mathbf{V}_i(k) \right. \\ & \left. + W_{\mathrm{d},i}(k)\hat{\mathbf{d}}_{p,i}(k)\right) + \lambda^T(k)\left(\tilde{\mathbf{u}}_\mathrm{t}(k) - \tilde{\mathbf{P}}_\mathrm{d}(k)\right) \\ & \text{subject to (11),} \end{aligned} \tag{23}$$

where $\tilde{\mathbf{u}}_\mathrm{t}(k)$ and $\tilde{\mathbf{P}}_\mathrm{d}(k)$ are the stacked versions of u_t and P_d over time steps k to $k + N_\mathrm{p}$. The variable $u_\mathrm{t}(k)$ represents the total power generation of FCEVs at time step k: $u_\mathrm{t}(k) = \sum_{i\in\mathcal{I}} u_{\mathrm{f},i}(k)$.

With a given value for $\lambda(k)$, the minimization part of (23) can be separated, i.e., distributed, between the FCEVs. For FCEV number $i \in \mathcal{I}$, the following problem should be solved:

$$\begin{aligned} \mathbf{V}_i^*(k) = \arg\min_{\mathbf{V}_i(k)} & \left(\mathbf{V}_i^T(k) W_{\mathrm{q},i}(k)\mathbf{V}_i(k) + W_{\mathrm{v},i}(k)\mathbf{V}_i(k) + W_{\mathrm{d},i}(k)\hat{\mathbf{d}}_{p,i}(k)\right) \\ & + \lambda^T(k)\tilde{\mathbf{u}}_{\mathrm{f},i}(k)\Big), \end{aligned} \tag{24}$$

subject to:

$$G_{1,i}(\hat{\mathbf{d}}_{p,i}(k))\mathbf{V}_i(k) \le G_{2,i}(k) + G_{3,i}(k)x_i(k), \quad \text{for } p \in \{1, \ldots, N\}. \tag{25}$$

All the optimization variables in (24) belong to a single FCEV and the problem can be solved without any dependencies on other FCEVs. The solution of (24) and (25), $\mathbf{V}_i^*(k)$, is in fact a function of $\lambda(k)$, where $\lambda(k + j)$ for $j \in \mathcal{P}$ can be interpreted as a signal to determine the need for power generation in different time steps. A lower value for $\lambda(k)$ indicates more need for power generation at time step k. The maximization part of (23) is called the master problem and can be written in the following form:

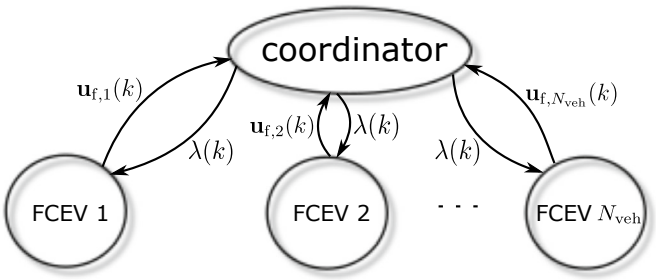

Fig. 1 Information exchanged between the coordinator and the FCEVs during one iteration at time step k using the dual decomposition approach

$$\max_{\lambda(k)\in\mathbb{R}^{N_{\mathrm{P}}}} \sum_{i\in\mathcal{I}} \mathbf{V}_i^*(\lambda(k)). \tag{26}$$

Note that $\sum_{i\in\mathcal{I}} \mathbf{V}_i^*(\lambda(k))$ is a concave function of $\lambda(k)$, because it is the minimum of a collection of linear functions in $\lambda(k)$. So, (26) can be solved by a gradient ascent algorithm. We consider a coordinator to solve the master problem (26). Note that only the variables related to the power generation, $u_{\mathrm{f},i}(k+j)$, for $i \in \mathcal{I}$ and $j \in \mathcal{P}$, are involved in the master problem (26) and, hence, driving patterns of the FCEVs, i.e., $\lambda_{\mathrm{f},i}(k+j)$, for $i \in \mathcal{I}$ and $j \in \mathcal{P}$, are not required for solving the master problem. Therefore, no privacy-sensitive data on usage of the FCEVs needs to be shared between the FCEVs and a central coordinator. The information exchanged between the coordinator and the FCEVs is demonstrated in Fig. 1.

ADMM Method

In the method of Alternating Direction Method of Multipliers (ADMM), the dual problem is constructed based on an augmented Lagrangian function, L_ρ [46]. By considering the definition of the cost function in (9) and the power balance constraint, the augmented Lagrangian function is of the following form:

$$L_\rho(\mathbf{u}(k), \mathbf{z}(k), \lambda) = J(k) + \lambda^T(\tilde{\mathbf{u}}_{\mathrm{t}}(k) - \tilde{\mathbf{P}}_{\mathrm{d}}(k)) + \frac{\rho}{2}||\tilde{\mathbf{u}}_{\mathrm{t}}(k) - \tilde{\mathbf{P}}_{\mathrm{d}}(k)||_2^2, \tag{27}$$

where ρ is a penalty parameter. The dual problem is then given by:

$$\begin{aligned} \mathrm{D}: \max_{\lambda\in\mathbb{R}^{N_{\mathrm{P}}}} \min_{\mathbf{u}(k),\mathbf{z}(k)} \; & L_\rho(\mathbf{u}(k), \mathbf{z}(k), \lambda) \\ \text{subject to } & (11). \end{aligned} \tag{28}$$

Based on the ADMM approach, in order to solve (28), each fuel cell requires to solve the following optimization problem:

$$\begin{aligned} &\min_{\mathbf{u}_i(k),\mathbf{z}_i(k)} \; L_{\rho,i}(\mathbf{u}_i(k), \mathbf{z}_i(k), \tilde{\mathbf{u}}_{\mathrm{r},i}(k), \lambda) \\ &\text{subject to (25)}, \end{aligned} \tag{29}$$

where $L_{\rho,i}$ and $\tilde{\mathbf{u}}_{\mathrm{r},i}(k)$ are defined as follows:

$$L_{\rho,i}(k,\lambda) = J_i(k) + \lambda^T(\tilde{\mathbf{u}}_{\mathrm{f},i}(k) + \tilde{\mathbf{u}}_{\mathrm{r},i}(k) - \tilde{\mathbf{P}}_{\mathrm{d}}(k)) + \frac{\rho}{2}||\tilde{\mathbf{u}}_{\mathrm{f},i}(k) + \tilde{\mathbf{u}}_{\mathrm{r},i}(k) - \tilde{\mathbf{P}}_{\mathrm{d}}(k)||_2^2$$
$$\tilde{\mathbf{u}}_{\mathrm{r},i}(k) = \left[\, u_{\mathrm{r},i}(k) \;\ldots\; u_{\mathrm{r},i}(k+N_{\mathrm{p}}-1) \,\right]^T.$$

In the above definition, $J_i(k)$ is a part of the cost function (7) related to fuel cell i and $u_{\mathrm{r},i}(k)$ is the total power generation of all the fuel cells except fuel cell i at time step k as follows:

$$J_i(k) = \sum_{j\in\mathcal{P}} \left(W_{\mathrm{p},i} u_{\mathrm{f},i}^2(k+j) + W_{\mathrm{s},i}|\Delta s_{\mathrm{f},i}(k+j)| + C_{\mathrm{e}}(k+j)d_i(k+j) \right),$$
$$u_{\mathrm{r},i}(k) = \sum_{n\in\mathcal{I}} u_{\mathrm{f},n}(k) - u_{\mathrm{f},i}(k).$$

If the value of $\tilde{\mathbf{u}}_{\mathrm{r},i}(k)$ is known for fuel cell i, (29) can be written as an MIQP problem

$$\begin{aligned} &\min_{\mathbf{V}_i(k)} \; \mathbf{V}_i^T(k) M_{\mathrm{q},i}(k) \mathbf{V}_i(k) + M_{\mathrm{v},i}(k)\mathbf{V}_i(k) \\ &\text{subject to (25)}, \end{aligned} \tag{30}$$

where $M_{\mathrm{q},i}(k)$ and $M_{\mathrm{v},i}(k)$ can be determined based on the model and driving pattern of FCEV i.

In the ADMM method, different agents solve their minimization problem one after another. In fact, each agent minimizes the augmented Lagrangian function by assuming that all the other agents have already made their decision. The determined solution, or the decision of the agent, will be shared with the next agent and the same procedure will be repeated until the last agent. After solving the last optimization problem, the coordinator will be informed about the decisions of all the agents. The coordinator executes a gradient ascent algorithm and, as a result, new values for the Lagrangian multipliers will be determined. The coordinator propagates these updated values among all the agents. In our problem formulation, only the power generation profiles of the fuel cells are involved in the global constraint. Therefore, there is no need to share all the optimization variables with other agents. It is worth mentioning that the driving patterns of the FCEVs can also be kept private, as they are not directly involved in the global constraint.

To solve the optimization problem (28) in a distributed fashion using the ADMM method, the following algorithm is executed at each time step k. First, the coordinator propagates an initial value for $\lambda(k)$ and all the FCEVs update the value of $\lambda(k)$ accordingly. Then, $\tilde{\mathbf{u}}_{\mathrm{t}}(k)$ is set to a zero vector of appropriate size and its value is transmitted to FCEV 1 to solve a minimization problem of the form (30) with $i = 1$. This agent later updates $\tilde{\mathbf{u}}_{\mathrm{t}}(k)$ according to the determined values for the optimization

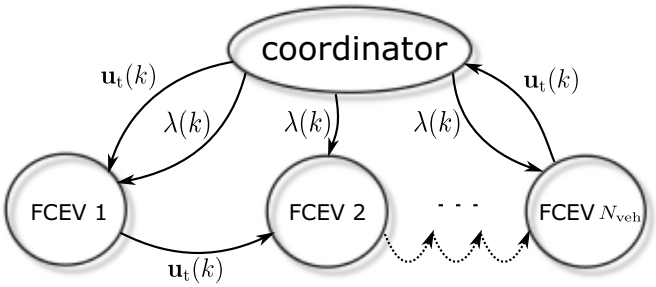

Fig. 2 Information exchanged between the coordinator and the FCEVs during one iteration at time step k using the ADMM approach

variables and passes it to the next agent. The same procedure is followed for each agent. The last agent sends back the updated value of $\tilde{\mathbf{u}}_{\mathrm{t}}(k)$ to the coordinator. Based on a gradient ascent algorithm and the new value of $\tilde{\mathbf{u}}_{\mathrm{t}}(k)$, the coordinator updates the value of $\lambda(k)$. At this point, the first iteration is completed. In the next iteration, the coordinator propagates $\lambda(k)$ to all the agents and sends the latest value of $\tilde{\mathbf{u}}_{\mathrm{t}}(k)$ to the first agent.

The next iterations are similar to the first one, except that each agent with number i subtracts the latest determined value for $\tilde{\mathbf{u}}_{\mathrm{f},i}(k)$ from $\tilde{\mathbf{u}}_{\mathrm{t}}(k)$ in order to determine the value of $\tilde{\mathbf{u}}_{\mathrm{r},i}(k)$. At the end of each iteration, the coordinator decides whether another iteration is required. The iterations are terminated in two cases: the current power schedule satisfies the power balance or the maximum number of iterations is reached. In the latter case, similar to the dual decomposition approach discussed before, the backup generation and storage units are used to compensate the error in the scheduled power. In any case, after termination of the iterations, all FCEVs pursue the power schedule determined at the last iteration until the next sampling time instant. Figure 2 demonstrates the exchange of information between the coordinator and the FCEVs.

PADMM Method

In the Proximal Alternating Direction Method of Multipliers (PADMM) [47], the coordinator and all the FCEVs are following the same procedure as described in previous sections. However, the optimization problem that is solved in the FCEVs is different because a proximal term is added to the objective function. In the ADMM method, the process of finding the optimal values for $\mathbf{u}(k)$ and $\mathbf{z}(k)$ is an iterative process, where at iteration $\kappa + 1$, the values of these variables are determined as follows:

$$\left(\mathbf{u}_i^{\kappa+1}(k)\ \mathbf{z}_i^{\kappa+1}(k)\right) = \underset{\mathbf{u}_i(k),\mathbf{z}_i(k)}{\arg\min}\ L\rho, i\ (\mathbf{u}_i(k), \mathbf{z}_i(k), \tilde{\mathbf{u}}_{\mathrm{r},i}(k), \lambda).$$

The calculation of the values for $\mathbf{u}(k)$ and $\mathbf{z}(k)$ at each iteration κ is done for a given value of λ, and it is independent of the calculations of the previous steps. The PADMM method differs from the ADMM method in how the optimization variables $\mathbf{u}(k)$ and $\mathbf{z}(k)$ are updated. In the PADMM method, a penalty term is added to the augmented Lagrangian function $L_{\rho,i}$ as follows:

$$\begin{pmatrix} \mathbf{u}_i^{\kappa+1}(k) \\ \mathbf{z}_i^{\kappa+1}(k) \end{pmatrix} = \underset{\mathbf{u}_i(k),\mathbf{z}_i(k)}{\arg\min}\ L_{\rho,i}(\mathbf{u}_i(k), \mathbf{z}_i(k), \tilde{\mathbf{u}}_{\mathrm{r},i}(k), \lambda) + \frac{\gamma}{\lambda}||\mathbf{u}_i(k) - \mathbf{u}_i^{\kappa}(k)||^2 + \frac{\gamma}{\lambda}||\mathbf{z}_i(k) - \mathbf{z}_i^{\kappa}(k)||, \tag{31}$$

where $\mathbf{u}_i^{\kappa}(k)$ and $\mathbf{z}_i^{\kappa}(k)$ are the values of $\mathbf{u}_i(k)$ and $\mathbf{z}_i(k)$ determined in the previous iteration κ. The addition of these new proximal terms will improve the convergence of the solution [47].

Using Eq. (31) and following a similar procedure as in the ADMM case, one can conclude that, rather than solving (30), fuel cell i solves the following problem during each iteration for time step k:

$$\begin{aligned} \min_{\mathbf{V}_i(k)}\ & \mathbf{V}_i^T(k) M_{\mathrm{q},i}(k)\mathbf{V}_i(k) + M_{\mathrm{v},i}(k)\mathbf{V}_i(k) \\ & + \tfrac{1}{2}(\mathbf{V}_i(k) - \mathbf{V}_i^{\mathrm{prev}}(k))^T Q_i(\mathbf{V}_i(k) - \mathbf{V}_i^{\mathrm{prev}}(k)) \\ \text{subject to } & (25), \end{aligned} \tag{32}$$

where $\mathbf{V}_i^{\mathrm{prev}}(k)$ indicates the vector of optimization variables related to agent i determined at the previous iteration. At the first iteration, we assume that $\mathbf{V}_i^{\mathrm{prev}}(k) = \mathbf{0}$. The matrix Q_i is a weight factor. The purpose of adding the proximal term to the objective function of each agent is to achieve a faster convergence compared to the ADMM method [47, 55]. Note that (32) is still an MIQP problem.

2.5 Illustrative Case Study

In this section, the results of simulating the developed control methods in a sample microgrid are reported. This section considers only an overview of the simulation results and the details of the simulated systems are not mentioned. All the results presented in this section are based on the work reported in [1] and the interested reader is referred to it for a detailed account of the simulations.

Table 1 lists the performance of the two developed centralized approaches, i.e., the min-max approach and the disturbance feedback min-max approach, for a microgrid containing four FCEVs. The microgrid is considered to be in the islanded mode with RESs. There is a base power generation profile for each FCEV. However, in order to maintain the power balance of the microgrid, the actual power generation of the FCEVs is uncertain. The difference between the actual and predicted power generation is considered as the disturbance here. The results of the simulation indicated

Table 1 Operational cost of a microgrid with a centralized control architecture using the disturbance feedback min-max (DF) approach and the min-max (MM) approach

N_p	4		6		8	
$\bar{\omega}_i$	MM	DF	MM	DF	MM	DF
0.5	2064	1819	2082	1876	2080	1901
1	2068	1762	2087	1754	2084	1852
1.5	2094	1699	2099	1508	2093	1483
2	2115	1454	2119	1511	2115	1553

that for different values of the prediction horizon, N_p, and the disturbance bound, $\bar{\omega}_i$, the disturbance feedback min-max approach outperforms the min-max approach. These results are as expected, because the level of conservatism in the disturbance feedback approach is less than in the min-max approach.

The simulation of the same microgrid is extended to incorporate the three distributed control approaches with the aim of comparing the performance of these control approaches. The operational cost of each distributed control approach is compared to that of the centralized solution in order to determine a measure for the loss of performance induced by the distributed solution. For example, if the operational cost of the system using the dual decomposition system is determined by J_{dd} and the centralized MPC cost is J_c, we define the performance loss, e_{dd}, as follows:

$$e_{dd} \triangleq \left| \frac{J_{dd} - J_c}{J_c} \right| \cdot 100\%.$$

A lower value for e_{dd} indicates that the performance of the dual decomposition approach is closer to the centralized solution. Similarly, we define two other measures for the performance loss, e_{admm} and e_{padmm}, related to the ADMM and PADMM approaches, respectively. Figure 3 depicts the performance loss for each distributed control method when the number of FCEVs is changing, for $N_p = 6$, and $\bar{\omega}_i = 1$. For the ADMM and PADMM methods, the performance loss drops significantly when the number of FCEVs in the system increases. In fact, when the number of FCEVs in the system increases, the influence of a single FCEV on the total power generation decreases. So, the influence of binary variables $s_{f,i}$ and $s_{r,i}$ for $i \in \mathcal{I}$, on the total power generation decreases when the number of FCEVs in the system increases. As a result, the optimization problem becomes more similar to a convex programming problem with the same form, but with continuous variables. We also know that in a convex programming problem the solutions of primal and dual problems are identical. This fact explains the decrease of performance loss in ADMM and PADMM when the number of FCEVs in the system increases. For a system with a small number of FCEVs, compared to the other distributed methods using the disturbance feedback min-max approach, the performance of PADMM is the closest to the one of the centralized solution.

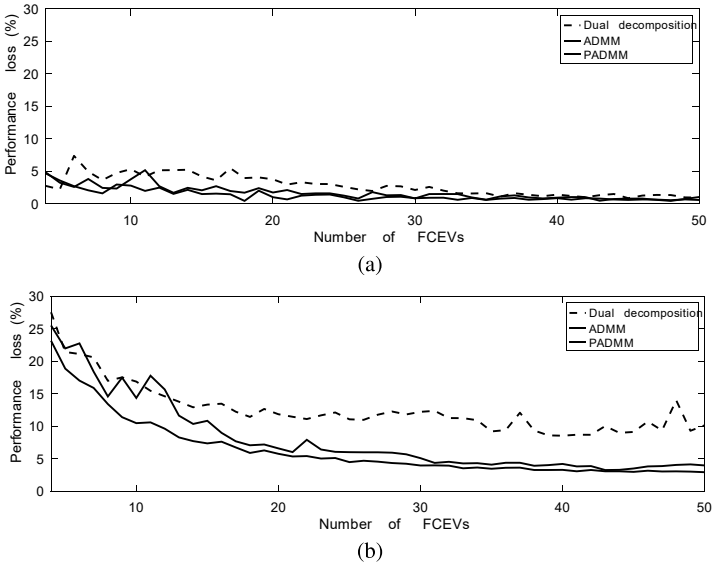

Fig. 3 Performance loss of distributed control systems, e_{dd}, e_{admm}, and e_{padmm}, with respect to the number of FCEVs inside the system for **a** the min-max approach and **b** the disturbance feedback min-max approach

In general, the reason for the performance loss in all the distributed methods is that for some time steps the power balance is achieved by using the auxiliary generators or batteries. In the distributed control architectures, two types of power generators or storage are used. The first type is the fleet of FCEVs and the second type is auxiliary generators or batteries. In the case that the power balance is not maintained by the FCEV, the auxiliary generators or batteries are used to maintain the power balance. As this auxiliary equipment is much more expensive to operate compared to FCEVs, in the case that there is a mismatch between the power generation of FCEVs and the residual load of the microgrid, the power balance is maintained by using the auxiliary equipment and, hence, the operational cost increases. The large performance loss of the dual decomposition method is mainly the result of a relatively high level of power imbalance after scheduling the power generation profile of all the FCEVs.

Table 2 lists the computation times of different control methods using various prediction horizons. This table shows that increasing the prediction horizon leads to a significant rise in the optimization time for all methods. However, across all cases, distributed control methods require less computation time compared to the centralized control method. Considering that the performance loss of the ADMM and PADMM methods is negligible in comparison to the centralized method for a CaPP system with a large number of vehicles, these methods can be deemed suitable for controlling a CaPP system.

Table 2 Computation time (in seconds) of different control strategies for a microgrid with 50 FCEVs, $\bar{\omega}_i = 0.5$, and for different values of N_p, using the min-max (MM) and the disturbance feedback min-max (DF) approaches

Method \ N_p	4	6	8
Centralized MM	1215	1608	2105
Dual decomposition MM	6	11	19
ADMM MM	188	347	607
PADMM MM	77	111	214
Centralized DF	1237	1620	2106
Dual decomposition DF	9	15	25
ADMM DF	421	702	1083
PADMM DF	189	301	503

3 Energy System Integration

The implementation of a CaPP system entails the integration of electricity and transportation systems. A fundamental distinction between current power grids and a prospective power grid based on FCEVs lies in the nature of power generation units. Up to recently, power grids consisted of large power plants operating relatively independently from other energy systems. The necessary fuel for these power plants served as the only link between the electricity network and other energy networks. Conversely, in a CaPP scenario, both the power generation units and their requisite fuel serve as the connecting elements.

In a CaPP scenario, where the power generation units and transportation means are the same, the electricity and transportation systems become interconnected. Consequently, a disturbance in one system will influence the other. For instance, the power generation capacity of parking lots for FCEVs depends on the number of FCEVs parked there. By utilizing historical data, one can estimate the number of vehicles for the foreseeable future and determine the power generation profile accordingly. However, in the event of a disturbance in the transportation network—such as extraordinary road congestion—the power generation capacity of FCEV parking lots will fluctuate, thereby affecting the electrical network.

Another significant difference between conventional power plants and parking lots for FCEVs in the CaPP system is the ownership of the equipment. A typical power plant is constructed solely for power generation, allowing all available information to be used in determining its power generation profile. However, for the CaPP system, electricity is generated via FCEVs, and the owners of these vehicles are individuals who may not be inclined to share sensitive information with third parties. An example of such sensitive information is the driving patterns of the FCEV owners. On the one hand, a parking lot requires access for the driving patterns of the FCEVs to estimate its power generation capacity; on the other hand, an FCEV owner may be

unwilling to share that information due to privacy concerns. A solution to this issue is the utilization of distributed control algorithms, as discussed in Sect. 2.4. However, employing distributed control algorithms necessitates increased communication between the parking lot and individual FCEVs, highlighting a crucial requirement of CaPP systems: the implementation of a secure and robust communication channel.

The primary concern regarding the communication channel is its security. Given that the CaPP system plays a pivotal role in maintaining the power balance of a microgrid, its reliable operation is of high importance. Consequently, the communication between the controller and the FCEVs must be safeguarded against potential attacks from malicious agents. Extensive research on the security of the communication process in the CaPP system is imperative before implementing such a system in real-world applications.

Another concern regarding communication is its reliability. Since the power planning algorithms depend on information from all FCEVs, the communication channel must be designed to minimize the likelihood of data packet losses and transfer delays. Additionally, the bandwidth of the communication channel should be sufficiently wide to accommodate a large fleet of FCEVs. Given the presence of multiple FCEV manufacturers, there is a necessity for a standardized communication protocol to ensure seamless integration of all FCEVs into the CaPP system. In Sect. 2, it has been assumed that a backup power generator is always available to compensate for any power imbalance. Consequently, occasional errors in communication between an FCEV and the control unit can be mitigated by the backup generator.

In a CaPP scenario, hydrogen plays a pivotal role as the primary energy source for both transportation and the electricity network. Consequently, the demand for hydrogen will be higher, given its usage across both energy networks. Any innovations in the production process and storage technology of hydrogen will directly impact the efficiency of both the electricity and transportation networks. To design an energy system based on the CaPP scenario with RESs as the main source of energy, one should consider the energy balance for both the electricity and the transportation systems. Interested readers are referred to [56] for an elaborated investigation on the shape of the hydrogen network, along with the development of a centralized optimization-based control algorithm.

4 Concluding Remarks and Future Research

In this chapter, we have considered a car as power plant (CaPP) system, in which a fleet of FCEVs is used to generate electricity inside a microgrid. The energy management system of the CaPP is able to schedule the power generation of these FCEVs and it is expected that this system maintains the power balance of the microgrid while there are uncertainties in the prediction of the microgrid's load or the number of FCEVs connected to the microgrid. To meet this expectation, we have developed MPC methods for the CaPP system in the presence of uncertainty. A min-max MPC method has been designed to guarantee the power balance of the system while the

operational cost of the system is minimized. In addition, we have developed three distributed MPC methods to increase the privacy of the FCEV owners regarding the driving patterns of the FCEVs.

Possible directions of future research are given as follows:

- **Minimizing the investment budget for realization of the first CaPP system**
  The real-life implementation of the system is of great importance and minimizing the investment budget for realization of the first CaPP system is an important element for a successful real-life implementation. The investment costs of different devices such as the DC to AC power converters, communication devices, and parking lots, should be analyzed.
- **Non-cooperative approach for distributed control**
  In the developed distributed control methods, we have assumed that all the agents, i.e., FCEVs, inside the system are cooperating with a coordinator. This assumption is not always true and there might be some special cases in which one or more agents are not cooperating with the coordinator. A control method should be developed for a CaPP system that can guarantee the power balance condition of the system in presence of such non-cooperative agents.
- **Market-based control**
  If we consider the non-cooperative behavior of the agents in the extreme case, i.e., when every agent is selfish and prefers the self benefit over the systems' performance, market-based control is a good candidate for the control system. A possible direction for the future research is the design of a market-based control algorithm for the CaPP system by considering the hard constraint of the power balance and the specific features of FCEVs such as a high level of cost for switching the fuel cell on or off, the limited fuel in each FCEV, and the transportation mode of the FCEVs.

References

1. Alavi F, van de Wouw N, De Schutter B (2020) Power scheduling of fuel cell cars in an islanded mode microgrid with private driving patterns. IEEE Trans Control Syst Technol 28(4):1393–1403
2. Alavi F, Lee EP, van de Wouw N, De Schutter B, Lukszo Z (2017a) Fuel cell cars in a microgrid for synergies between hydrogen and electricity networks. Appl Energy 192:296–304
3. Walters M, Kuhlmann A, Ogrzewalla J (2015) Fuel cell range extender for battery electric vehicles. In: International conference on electrical systems for aircraft, railway, ship propulsion and road vehicles (ESARS), Aachen, Germany
4. Gou B, Na WK, Diong B (2009) Fuel cells: modeling, control, and applications. CRC Press
5. Lipman TE, Elke M, Lidicker J (2018) Hydrogen fuel cell electric vehicle performance and user-response assessment: results of an extended driver study. Int J Hydrog Energy 43(27):12442–12454
6. Samuelsen S (2017) The automotive future belongs to fuel cells: range, adaptability, and refueling time will ultimately put hydrogen fuel cells ahead of batteries. IEEE Spectr 54(2):38–43

7. Lukszo Z, Farahani S (2021) A comprehensive engineering approach to shaping the future energy system. Springer International Publishing. ISBN 978-3-030-74586-8
8. Holttinen H, Tuohy A, Milligan M, Lannoye E, Silva V, Müller S, Söder L (2013) The flexibility workout: managing variable resources and assessing the need for power system modification. IEEE Power Energy Mag 11(6):53–62. ISSN 1540-7977
9. Wolsink M (2012) The research agenda on social acceptance of distributed generation in smart grids: renewable as common pool resources. Renew Sustain Energy Rev 16(1):822–835
10. Verzijlbergh RA, Lukszo Z, Ilic MD (2012) Comparing different EV charging strategies in liberalized power systems. In: International conference on the European energy market, pp 1–8
11. Lipman TE, Edwards JL, Kammen DM (2004) Fuel cell system economics: comparing the costs of generating power with stationary and motor vehicle PEM fuel cell systems. Energy Policy 32(1):101–125
12. Kissock JK (1998) Combined heat and power for buildings using fuel-cell cars. In: Proceedings of the ASME international solar energy conference, pp 121–132
13. Farahani S, Bleeker C, van Wijk A, Lukszo Z (2020) Hydrogen-based integrated energy and mobility system for a real-life office environment. Appl Energy 264:114695
14. van Wijk AJM, Verhoef L (2014) Our car as power plant. Delft University Press. ISBN: 9781614993766
15. Fernandes A, Woudstra T, van Wijk A, Verhoef L, Aravind PV (2016) Fuel cell electric vehicle as a power plant and SOFC as a natural gas reformer: an exergy analysis of different system designs. Appl Energy 173:13–28
16. Parhizi S, Lotfi H, Khodaei A, Bahramirad S (2015) State of the art in research on microgrids: a review. IEEE Access 3:890–925
17. Hou L, Dong J, Herrera OE, Mérida W (2023) Energy management for solar-hydrogen microgrids with vehicle-to-grid and power-to-gas transactions. Int J Hydrog Energy 48(5):2013–2029
18. Conejo AJ, Wu X (2022) Robust optimization in power systems: a tutorial overview. Optim Eng 23(4):2051–2073
19. Narayan A, Ponnambalam K (2017) Risk-averse stochastic programming approach for microgrid planning under uncertainty. Renew Energy 101:399–408
20. Khodr HM, El Halabi N, García-Gracia M (2012) Intelligent renewable microgrid scheduling controlled by a virtual power producer: a laboratory experience. Renew Energy 48:269–275
21. Battistelli C (2013) Generalized microgrid-to-smart grid interface models for vehicle-to-grid. In: PES innovative smart grid technologies conference, pp 1–6
22. Shinoda K, Lee EP, Nakano M, Lukszo Z (2016) Optimization model for a microgrid with fuel cell vehicles. In: 13th IEEE international conference on networking, sensing and control (ICNSC), pp 1–6
23. Vidueira JM, Contreras A, Veziroglu TN (2003) PV autonomous installation to produce hydrogen via electrolysis, and its use in FC buses. Int J Hydrog Energy 28(9):927–937
24. Schiffer J, Ortega R, Astolfi A, Raisch J, Sezi T (2014) Conditions for stability of droop-controlled inverter-based microgrids. Automatica 50:2457–2469
25. Schiffer J, Zonetti D, Ortega R, Stanković AM, Sezi T, Raisch J (2016) A survey on modeling of microgrids—from fundamental physics to phasors and voltage sources. Automatica 74:135–150
26. Kammer C, Karimi A (2017) Decentralized and distributed transient control for microgrids. IEEE Trans Control Syst Technol 1–12
27. Guerrero JM, Vasquez JC, Mata J, de Vicuña LG, Castilla M (2011) Hierarchical control of droop-controlled AC and DC microgrids—a general approach toward standardization. IEEE Trans Ind Electron 58(1):158–172
28. Cortes A, Martinez S (2015) A hierarchical demand-response algorithm for optimal vehicle-to-grid coordination. In: European control conference (ECC), Linz, Austria, pp 2425–2430
29. Arnold M, Negenborn RR, Andersson G, De Schutter B (2009) Multi-area predictive control for combined electricity and natural gas systems. In: European control conference (ECC), pp 1408–1413

30. Montero L, Bello A, Reneses J (2022) A review on the unit commitment problem: approaches, techniques, and resolution methods. Energies 15(4)
31. Padhy NP (2004) Unit commitment-a bibliographical survey. IEEE Trans Power Syst 19(2):1196–1205 May
32. Peng C, Lei S, Hou Y, Wu F (2015) Uncertainty management in power system operation. CSEE J Power Energy Syst 1(1):28–35 March
33. Prodan I, Zio E (2014) A model predictive control framework for reliable microgrid energy management. Electr Power Energy Syst 61:399–409
34. del Real AJ, Arce A, Bordons C (2007) Hybrid model predictive control of a two-generator power plant integrating photovoltaic panels and a fuel cell. In: 46th IEEE conference on decision and control, pp 5447–5452
35. Zhang L, Gari N, Hmurcik LV (2014) Energy management in a microgrid with distributed energy resources. Energy Convers Manag 78:297–305
36. Parisio A, Rikos E, Glielmo L (2014) A model predictive control approach to microgrid operation optimization. IEEE Trans Control Syst Technol 22(5):1813–1827
37. Ghotge R, Snow Y, Farahani S, Lukszo Z, van Wijk A (2020) Optimized scheduling of EV charging in solar parking lots for local peak reduction under EV demand uncertainty. Energies 13(5)
38. Hans CA, Nenchev V, Raisch J, Reincke-Collon C (2014) Minimax model predictive operation control of microgrids. In: The 19th world congress of the international federation of automatic control, Cape Town, South Africa, pp 10287–10292
39. Parisio A, Glielmo L (2013) Stochastic model predictive control for economic/environmental operation management of microgrids. In: European control conference (ECC), Zürich, Switzerland, pp 2014–2019
40. Guan Y, Wang J (2014) Uncertainty sets for robust unit commitment. IEEE Trans Power Syst 3(29):1439–1440
41. Bertismas D, Litvinov E, Sun XA, Zhao J, Zheng T (2013) Adaptive robust optimization for the security constrained unit commitment problem. IEEE Trans Power Syst 28(1):52–63
42. Mesbah A (2016) Stochastic model predictive control: an overview and perspectives for future research. IEEE Control Syst Mag 36(6):30–44
43. van Hessem DH, Bosgra OH (2003) A full solution to the constrained stochastic closed-loop MPC problem via state and innovations feedback and its receding horizon implementation. In: 42nd IEEE conference on decision and control, pp 929–934
44. Longson W, Chryssochoos I, Raković SV, Mayne DQ (2004) Robust model predictive control using tubes. Automatica 40:125–133
45. Bertsekas DP (1999) Nonlinear programming. Athena Scientific
46. Boyd S, Parikh N, Chu E, Peleato B, Eckstein J (2011) Distributed optimization and statistical learning via the alternating direction method of multipliers. Found Trends Mach Learn 3(1):1–122
47. Eckstein J (1994) Some saddle-function splitting methods for convex programming. Optim Methods Softw 4(1):75–83
48. Rodatz P, Paganelli G, Sciarretta A, Guzzella L (2005) Optimal power management of an experimental fuel cell/supercapacitor-powered hybrid vehicle. Control Eng Pract 13(1):41–53
49. Bemporad A, Morari M (1999) Control of systems integrating logic, dynamics, and constraints. Automatica 35(3):407–427
50. Gross G, Galiana FD (1987) Short-term load forecasting. Proc IEEE 75(12):1558–1573
51. Alavi F (2019) Model Predictive Control of fuel-cell-Car-based smart energy systems in the presence of uncertainty. PhD thesis, Delft University of Technology
52. CPLEX. CPLEX optimizer. https://www.ibm.com/products/ilog-cplex-optimization-studio/cplex-optimizer
53. Gurobi. Gurobi optimization. https://www.gurobi.com/
54. Alavi F, van de Wouw N, De Schutter B (2017b) Power scheduling in islanded-mode microgrids using fuel cell vehicles. In: 56th IEEE conference on decision and control, Melbourne, Australia, pp 5056–5061

55. Wang JJ, Song W (2017) An algorithm twisted from generalized ADMM for multi-block separable convex minimization models. J Comput Appl Math 309:342–358
56. Farahani SS, van der Veen R, Oldenbroek V, Alavi F, Lee EHP, van de Wouw N, van Wijk A, De Schutter B, Lukszo Z (2019) Hydrogen-based integrated energy and transport system. IEEE Syst Man Cybern Mag 5(1):37–50